Image Fusion in Remote Sensing Applications: A Review

Vaibhav R. Pandit
Research Scholar
S.G.B. Amravati University,
Amravati, India

R. J. Bhiwani, PhD
Professor
B.N. College of Engineering,
Pusad, India

ABSTRACT
Major technical constraints like minimum data storage at satellite platform in space, less bandwidth for communication with earth station, etc. limits the satellite sensors from capturing images with high spatial and high spectral resolutions simultaneously. To overcome this limitation, image fusion has proved to be a potential tool in remote sensing applications which integrates the information from combinations of panchromatic, multispectral or hyperspectral images; intended to result in a composite image having both higher spatial and higher spectral resolutions. The research in this area cites date back to last few decades, but the diverse approaches proposed so far by different researchers have been rarely discussed at one place. This paper is an honest attempt to collectively discuss all possible algorithms along with quality metrics following two assessment procedures i.e. at full and reduced scale resolutions to evaluate performance of these algorithms.

General Terms
Remote sensing, Image fusion, Satellite image processing.

Keywords
Image fusion, Relative spectral contribution methods, Component substitution, Multiresolution analysis, Quality metrics for performance evaluation.

1. INTRODUCTION
A wide variety of remotely sensed data products like panchromatic (PAN), multispectral (MS), hyperspectral (HS), synthetic aperture radar (SAR) imagery, etc. covering different parts of electromagnetic spectrum are made available by different earth observation satellites. These remote sensing data products are further processed and used for crop production forecast, forest cover and type mapping, mineral/oil exploration, weather prediction, watershed development and monitoring, urban sprawl mapping of major cities, disaster management, etc. [1]. Fig. 1 shows flow of tasks in remote sensing image processing. For many of the applications listed, image analysis of only one source type is insufficient. For detail understanding of the observed earth surface, it is better to get complementary information from more than one sensor. Thus, image fusion becomes the best option to integrate information collected from different imaging sensors at different spectral, spatial, temporal and radiometric resolutions [2] [3]. Image fusion is a subset of more diverse research area 'data fusion' which is defined as: "Data fusion is a formal framework in which are expressed means and tools for the alliance of data originating from different sources. It aims at obtaining information of greater quality; the exact definition of 'greater quality' will depend upon the application" [4]. Image fusion takes place at three different levels.

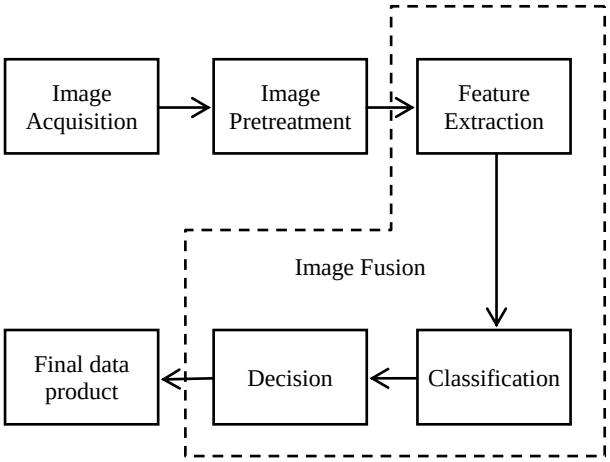

Fig 1: Remote sensing image processing.

1.1 Pixel Level Image Fusion
Pixel-level image fusion is the lowest level of image fusion, where a new image is formed having pixel values obtained by combining the pixel values of different images through some algorithms under strict registration conditions [5]. The new image keeps more raw data to provide rich and accurate image information which is further used for easy analysis and processing by feature extraction and classification. The image fusion at pixel level may be single sensor, multi-sensor or temporal image fusion, etc. Advantage of pixel-level image fusion is minimum loss of information, but it has the largest amount of information to be processed, thus slowest processing speed, and a higher demand for equipment [6] [7] [8].

1.2 Feature Level Image Fusion
Feature-level fusion is intermediate level of image fusion where the features (edges, texture, shape, spectrum, angle or direction, speed, similar lighting area, similar depth of focus area, etc.) generally in statics are extracted from different images of the same geographical area by separate preprocessing [6]. The extracted features are combined to form an optimum feature set, further classified using statistical or other types of classifiers. Features from different source-images preprocessed using different schemes are combined to form a decision [7].

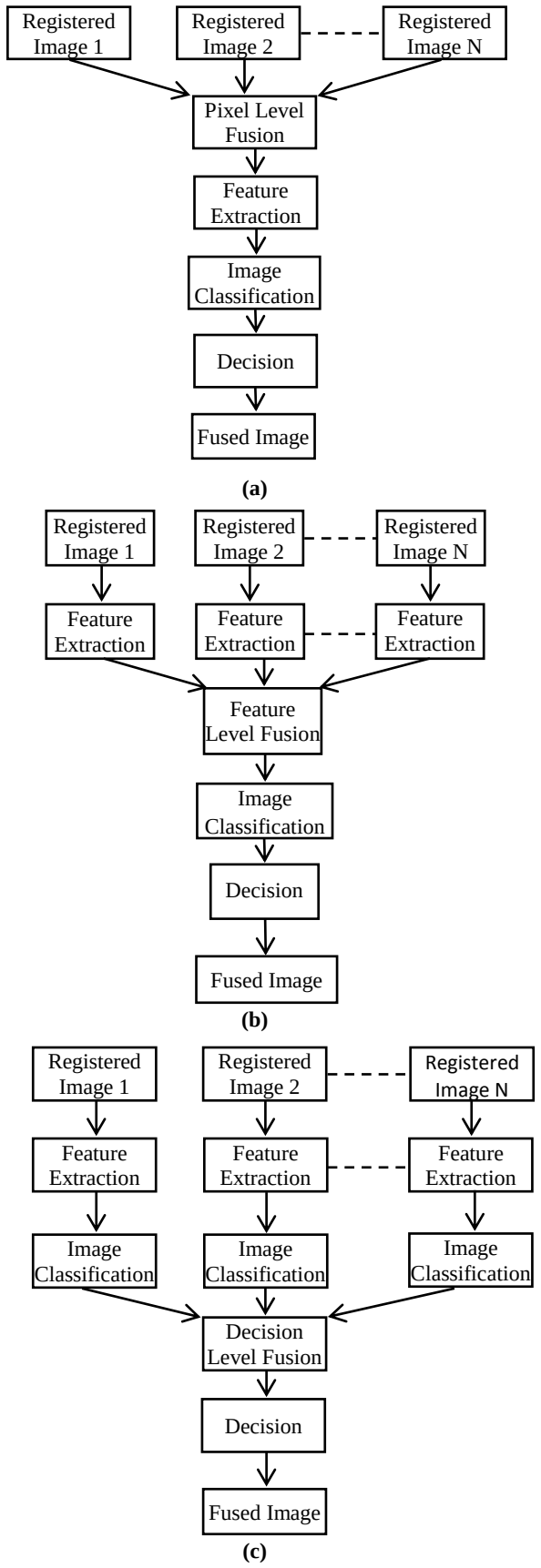

Fig 2: (a) Scheme of pixel level fusion, (b) Scheme of feature level fusion, (c) Scheme of decision level fusion.

Here, correlative feature information is excavated, redundant features are eliminated and new compound features are established, increasing the degree of reliability of feature information. The requirement of sensor alignment in feature-level fusion is less strict than pixel-level's. So, image sensors can be distributed in different platforms. The advantages of feature-level fusion are that it achieved considerable compression of information, it is conducive to real-time processing and its fusion results can further give the feature information for decision analysis. Here, the extracted features are directly related to the decision analysis [5] [8].

1.3 Decision Level Image Fusion

Decision-level fusion is a high-level fusion, and its results provide the basis for command and control decision making. In decision-level fusion, the images are processed separately [5]. The processed information is then refined by combining the information obtained from different sources and the differences in information are resolved based on certain decision rules. In literature, two types of decision level fusion are observed. Here, classification from different types of classifiers for the same image may be combined to get better classification accuracies or two different complimentary sources like optical imagery and radar data can be classified separately and combined to produce a refined classification map [8]. A variety of logical reasoning methods, statistical methods, information theory methods can be used for decision-level fusion, such as Bayesian reasoning, D-S (Dempster-Shafer) evidence reasoning, voting system, cluster analysis, fuzzy set theory, neural network , the entropy method and so on. Decision-level fusion has a good real-time and fault tolerance, but its pretreatment cost is higher. The data quantity of decision-level fusion is the smallest and its ability of anti-interference is the highest. The probability and reality of fused results are high and the performance of multi-sensor system is improved [6] [7]. Accompanied Fig. 2 shows image fusion schemes at three different levels.

The remainder of the paper is organized as follows: Section II presents a brief review of some of the image fusion approaches published earlier. Section III is devoted to image fusion methods belonging to different approaches, providing a detailed description of some algorithms. Section IV describes quality metrics for the evaluation of image fusion performance based on two assessment procedures operating at reduced and full resolutions. Future scope and limitations of the research are discussed in Section V. Finally, conclusions are drawn in Section VI.

2. LITERATURE REVIEW

To know the current state of art of image fusion in remote sensing, this section reviews some of the research papers published earlier.

For fusion of MS image with PAN image (also called as pansharpening), it is observed that the effective high quality is achieved with the expense of large computational complexity, more time consumption and difficulties to process large size images. Along with this, Gemine Vivone *et al.* in [9] focused some important points as: the lack of universally recognized evaluation criteria, unavailability of image data sets for benchmarking and absence of standardized implementations of the algorithms to make a thorough evaluation and comparison of the different pansharpening methods. Pansharpening algorithms belonging to the two more established and addressed categories viz. component substitution (CS) and multiresolution analysis (MRA) are considered by authors to be evaluated and compared over five

data sets acquired by different satellites. Wenqing Wang *et al.* [10] further propose an adaptive component substitution based pansharpening, adopting a particle-swarm-optimization algorithm to solve the single objection optimization problem. The proposed framework is compared with popular CS based methods based on correlation coefficient, mutual information and mean-structural-similarity index. Andrea Garzelli *et al.* [11] while extending this classical component-substitution approach, propose to develop a fast nonlocal parameter based pansharpening method *K*-means clustering and overcoming window-based local estimation. In a try to solve the problem of color distortion, Qizhi Xu *et al.* [12] divides the pixels of PAN and MS images into several classes by *k*-means algorithm followed by multiple regression to calculate summation weights on each group of pixels. It is also noticed that due to the nonlinear spectral response of satellite sensors, synthesis of low-resolution PAN image required in some methods cannot be well approximated resulting in color distortion.

Image fusion methods based on filters are also popular, where spatial information from the PAN image is extracted and injected into MS images. Hamid Reza Shahdoosti *et al.* in [13] address the designing of optimal filter that is able to extract relevant and non-redundant information from the PAN image. The performance is statistically evaluated using correlation coefficient (CC), relative dimensionless global error in synthesis (ERGAS), spectral angle mapper (SAM), universal image quality index (UIQI) and quality without reference (QNR). Using Discrete Wavelet Transform (DWT), there are no constraints about details that can be extracted from PAN and because of lack of orthogonality; Abdelaziz Kallel *et al.* [14] propose a coupled multiresolution decomposition model (CMD) fusion scheme. Kishor P. Upla *et al.* in [15] proposes a more advanced multiresolution fusion approach using contourlet transform (CT), by modeling the MS image as the degraded and noisy version of its high spatial resolution version, an ill-posed problem. Expecting better directionality from CT for initial estimate, authors demonstrate the approach using subsampled and non-subsampled CT on data sets from Quickbird, IKONOS-2 and Worldview-2 satellites. Also, to find the functional relation between the PAN and MS images by typical modulation transfer function of the MS sensor which is many times approximated as a Gaussian filter is often inadequate for pansharpening. Hence, Gemine Vivone *et al.* in [16] tried to develop an efficient optimization procedure with semiblind deconvolution approach. The approach has been validated with datasets from IKONOS and QuickBird at reduced and full scale resolution over Q4, SAM, ERGAS, etc. Syed Muhammad Umer Abdullah *et al.* [17] proposes a class of schemes for the pansharpening of multispectral (MS) images using multivariate empirical mode decomposition (MEMD) algorithm, an extension of the empirical mode decomposition (EMD) algorithm, which tries to overcome mode-mixing, nonuniqueness, mode misalignment issues of the EMD and enabling the decomposition of multivariate data into its intrinsic oscillatory scales. Huihui Song *et al.* in [18] present a learning based super-resolution method to fuse Landsat Thematic Mapper (TM)/Enhanced Thematic Mapper Plus (ETM+) images with Système Pour l'Observation de la Terre 5 (SPOT5) images, taking advantages of wide swath width of the former and the high spatial resolution of the latter. The imaging process is modeled from a SPOT to TM/ETM+ image by image degradation via blurring and downsampling operations. Simulated Landsat image thus avoids geometric coregistration. Further, classification experiments are demonstrated on fusion result and actual images. The application of sparse representation (SR) theory to the fusion of MS and PAN images is also observed in literature, where estimation of missing details that are to be injected in the available MS image to enhance its spatial features is done. Maria Rosaria Vicinanza *et al.* [19] presents implementation of the technique on datasets from WorldView-2 and IKONOS sensors, with comparison of classical pansharpening methods at reduced and full resolutions.

Other than fusion of MS with PAN image, fusion of MS with HS images is also seen in literature. Due to complexity and cost issues, MS and HS images have different resolutions with significantly lower spatial resolution than that of PAN images. HS remote sensing images have advantage of more information content due to large number of bands involved, but the same time its application has been constrained due to the narrow swath width. Thus, a fusion of HS and MS images is proposed many times. Miguel Simões *et al.* [20] formulate this data fusion problem as the minimization of blur, additive noise, etc. promoting piecewise-smooth solutions. Author estimate a hard estimation problem in accounting different spatial resolutions, handling very large size of HS image together, etc. which is performed by following an Alternating Direction Method of Multipliers (ADMM) approach and using the Split Augmented Lagrangian Shrinkage Algorithm (SALSA). Here, a blind approach focusing the inherent data redundancy to achieve better results is followed. Xuejian Sun *et al.* in [21] proposes a spectral resolution enhancement method (SREM) for remotely sensed MS image, to generate wide swath HS images using auxiliary multi/hyper-spectral data. Transformation matrices are generated followed by a spectral angle weighted minimum distance (SAWMD) matching method to create HS vectors from the original MS image, pixel by pixel. Further Caroline M. Gevaert *et al.* in [22] performs fusion of MS and HS images acquired with Formosat- 2 and an unmanned aerial vehicle (UAV) respectively to construct Spectral–temporal response surfaces (STRSs) providing continuous reflectance spectra at high temporal intervals for precision agriculture requirements. The method uses Bayesian theory to impute missing spectral information in the MS imagery. The performance of method is evaluated on field measured reflectance spectra, leaf area index (LAI), etc. On the other hand, Qi Wei *et al.* in [23] present an approach for fusing HS and MS images based on sparse representation. An inverse problem of image fusion is formulated, assuming the target image to live in a lower dimensional subspace. Dictionary learning with design of a sparse regularization term are done and results are simulated for comparison to preexisting methods. To enhance spatial resolution of MS and HS images, Frosti Palsson *et al.* [24] proposes a method for fusion of MS or HS with PAN images and MS with HS images. Spectral redundancy is tried to be reduced by principal component analysis (PCA) and use of wavelets. The approach is said to have benefits of substantially lower computational requirements and very high tolerance to noise for WorldView-2 data.

Image fusion has wide application area. Claudia Paris *et al.* in [25], based on the fusion between low-density LiDAR (Light detection and ranging) data and high-resolution optical images proposes a 3-D model-based approach to the estimate tree top height as one of the forest attributes. While, Wenzhi Liao *et al.* in [26] propose a *generalized* graph-based fusion method to couple dimension reduction and feature fusion of hyperspectral and LiDAR data. The edges of the fusion graph are weighted by the distance between the stacked feature points. Difficulties and ambiguities in object recognition of

urban areas are tried to be avoided by Fatemeh Tabib Mahmoudi *et al.* in [27]. The authors propose object-based image analysis (OBIA) to be performed in case of single view processes; while in multiviews' case, all the views are to be fused at decision level. The approach is implemented to produce results for WorldView-2 and the digital modular camera (DMC) datasets. Network transmissions for surveillance in radar systems are generally narrowband. Gianluca Gennarelli *et al.* [28] propose to use single-frequency approach for imaging targets with passive arrays deployed around the scattering scene. Employing a multiarray image fusion strategy in conjunction with a change detection scheme for imaging moving targets, better resolution images are obtained. The author carries some numerical estimation using this approach. Yong Xu *et al.* [29] develop a spatial and temporal data fusion model based on regularized spatial unmixing to generate Landsat-like synthetic data and the high temporal resolution of Moderate Resolution Imaging Spectro-radiometer (MODIS) data. After considering the neighborhood size of the MODIS data, the number of classes of Landsat data for spatial unmixing and a regularization parameter added to the cost function to reduce unmixing error the approach is evaluated by calculating ERGAS. Wei Li *et al.* [30] propose a classification paradigm to exploit rich texture information of HS image. The framework employs local binary patterns (LBPs) to extract features such as edges, corners and spots. Feature-level fusion and decision-level fusion are applied to the extracted LBP features before classification.

3. IMAGE FUSION METHODS

Many methods for image fusion are reported in literature. The methods for pansharpening can be broadly categorized in three major groups as: relative spectral contribution methods, projection substitution (also called component substitution (CS)) methods and the methods belonging to ARSIS (Amélioration de la Résolution Spatiale par Injection de Structures) concept. The latter group of methods is sometimes also referred to as multiresolution analysis (MRA) methods. The methods showing resemblance to more than one group may be treated as Hybrid methods. Brovey transform (BT), Synthetic variable ratio (SVR) and Ratio enhancement (RE) are some examples of relative spectral contribution methods. CS methods include Intensity-Hue-Saturation (IHS) transform, principal component analysis (PCA) and Gram-Schmidt (GS), etc. The powerful and dynamic wavelet transform based methods and its extensions perform multiresolution analysis. Fig. 3 represents evolution of image fusion methods for remote sensing. Some selected methods from the three groups are discussed in following subsections.

3.1 Average

It is a well-documented fact that regions of images that are in focus tend to be of higher pixel intensity. Thus, this algorithm is a simple way of obtaining an output image with all regions in focus. In this method the resultant fused image is obtained by taking the average intensity of corresponding pixels from both the input image [31].

$$F_{ij} = \frac{(A_{ij} + B_{ij})}{2} \qquad (1)$$

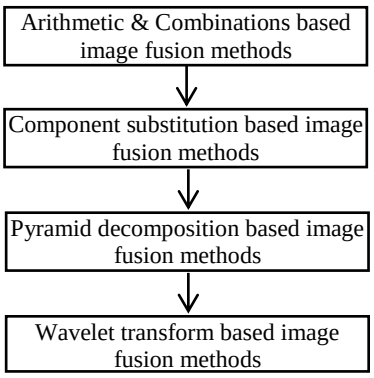

Fig 3: Evolution of image fusion methods.

3.2 Select Maximum

The greater the pixel values the more in focus the image. Thus this algorithm chooses the in-focus regions from each input image by choosing the greatest value for each pixel, resulting in highly focused output. In this method, the resultant fused image is obtained by selecting the maximum intensity of corresponding pixels from both the input images [31].

$$F_{ij} = \sum_{i=0}^{m} \sum_{j=0}^{n} \max A_{ij}\, B_{ij} \qquad (2)$$

3.3 Select Minimum

In this method, the resultant fused image is obtained by selecting the minimum intensity of corresponding pixels from both the input images [31].

$$F_{ij} = \sum_{i=0}^{m} \sum_{j=0}^{n} \min A_{ij}\, B_{ij} \qquad (3)$$

For equations (1), (2) and (3), A_{ij} and B_{ij} are input images to be fused, while F_{ij} is resultant fused image.

3.4 Multiplicative Method

This method performs pixel to pixel multiplication of low spatial resolution multispectral image with high spatial resolution panchromatic image [32]. This simple method can be formulated as:

$$Red = (LR_1 * HR_1) \qquad (4)$$

$$Green = (LR_2 * HR_2) \qquad (5)$$

$$Blue = (LR_3 * HR_3) \qquad (6)$$

Here, LR = Low spatial resolution MS band, HR = High spatial resolution PAN band.

3.5 Brovey Transform

The Brovey transform (BT) is a numerical fusion method which is based on Chromaticity transform. It focuses on fusing the images while preserving the colors of the original optical image. The BT uses a mathematical combination of the MS bands and PAN band. Each MS band is multiplied by a ratio of the PAN band divided by the sum of the MS bands. Its purpose is to normalize the three MS bands and to add the intensity or brightness component to the image [33]. It is a simple method for combining data from different sensors, with the limitation that only three bands are involved [4]. Successful application of this technique requires an experienced analyst for the specific adaptation of parameters. It is given by:

$$Red = \frac{Band_1}{\sum_{i=1}^{n} Band_n} * HR\ Band \qquad (7)$$

$$Green = \frac{Band_2}{\sum_{i=1}^{n} Band_n} * HR\ Band \qquad (8)$$

$$Blue = \frac{Band_3}{\sum_{i=1}^{n} Band_n} * HR\ Band \qquad (9)$$

3.6 Intensity-Hue-Saturation (IHS)

The intensity-hue-saturation (IHS) method is a standard procedure in the area of image fusion having fast computing capability for fusing images. Digital images in computer are generally displayed by an additive color composite system using the three primary colors – red (R), green (G) and blue (B). Since, perception of colors to humans always recognize with three features – intensity (I), hue (H) and saturation (S), the IHS fusion method converts a color multispectral (MS) image from the RGB space into the IHS color space [34]. While the RGB is a rectangular coordinate system and IHS is a cylindrical coordinate system, the conversion is performed by rotation of axis from the orthogonal RGB system to a new orthogonal IHS system [35]. The intensity represents the overall brightness or luminance of the scene of any color, the hue component refers to dominant wavelength of the light contributing to the scene and saturation component describes its purity. Most literature recognizes IHS as a third-order method because it employs a 3×3 matrix in its transform kernel. The appearance of the panchromatic (PAN) image is similar to the intensity band of an IHS representation of the scene. Therefore, during fusion i.e. pan-sharpening, the MS image is projected onto the IHS color space and the intensity band is replaced by the PAN image. The fusion output can then be obtained by the reverse IHS transform [36]. The steps in IHS method are given below, where the equations (10), (11), (12) give mathematical interpretations of forward transformation while equation (13) gives IHS reverse transformation.

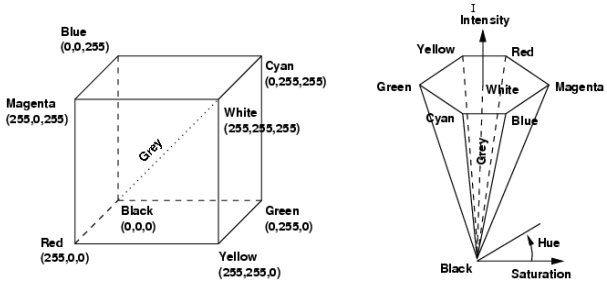

Fig 4: RGB to IHS color transformation.

1. The low resolution MS imagery is co-registered to the same area as the high resolution PAN imagery and resampled to the same resolution as the PAN imagery. It is generally performed using bi-cubic interpolation.
2. The three resampled bands of the MS imagery, which represent the RGB space are transformed into IHS components. It is mathematically represented as follows-

$$\begin{bmatrix} I \\ V_1 \\ V_2 \end{bmatrix} = \begin{bmatrix} \frac{1}{3} & \frac{1}{3} & \frac{1}{3} \\ \frac{1}{\sqrt{6}} & \frac{1}{\sqrt{6}} & \frac{-2}{\sqrt{6}} \\ \frac{1}{\sqrt{2}} & \frac{-1}{\sqrt{2}} & 0 \end{bmatrix} \begin{bmatrix} R \\ G \\ B \end{bmatrix} \quad (10)$$

$$H = \tan^{-1}\left(\frac{V_2}{V_1}\right) \quad (11)$$

$$S = \sqrt{{V_1}^2 + {V_2}^2} \quad (12)$$

Where, V_1 and V_2 are intermediate variables.

3. The PAN imagery is histogram matched to the 'I' component. This is done in order to compensate for the spectral differences between the two images, which occurred due to different sensors or different acquisition dates and angles.
4. The intensity component of MS imagery is replaced by the histogram matched PAN imagery. The RGB of the new merged MS imagery is obtained by computing a reverse IHS to RGB transform. Following equation gives IHS inverse transform.

$$\begin{bmatrix} R \\ G \\ B \end{bmatrix} = \begin{bmatrix} 1 & \frac{1}{\sqrt{6}} & \frac{1}{\sqrt{2}} \\ 1 & \frac{1}{\sqrt{6}} & \frac{-1}{2} \\ \frac{11}{\sqrt{2}} & \frac{-2}{\sqrt{6}} & 0 \end{bmatrix} \begin{bmatrix} I \\ V_1 \\ V_2 \end{bmatrix} \quad (13)$$

3.7 Principal Component Analysis (PCA)

When the number of images to be fused is higher than three i.e. fusion of multidimensional data, principal component analysis (PCA) a statistical tool (which is also known as Karhunen-Lo´eve transform) is used for dimensionality reduction [37]. In the most common understanding, PCA is a data compression technique transforming the intercorrelated data into a new set of uncorrelated components (PC_1, PC_2, … , PC_n, where n is the number of input multispectral bands) which is often more interpretable than the source data. It computes the basis vectors by analyzing the direction of maximum data variance and projects the data onto them. For PCA based image fusion, the principle components of the MS image bands are calculated. The first principle component which contains the most information of the image resembles with the panchromatic image and hence is substituted by the panchromatic data. Finally the inverse principal component transform is done to get the new RGB bands of sharpened multi-spectral image from the principle components [38].

To understand PCA, a two dimensional histogram which forms an ellipse is considered. Here the axes of the spectral space are rotated, changing the coordinates of each pixel in spectral space. The new axes are parallel to the axes of the ellipse. The widest transect, which corresponds to the major axis of the ellipse, is called the first principal component (PC_1) of the data. The direction of the first principal component is the first eigenvector and its length is the first eigenvalue. The second principal component (PC_2) is the widest transect of the ellipse corresponding to minor axis that is perpendicular to the first principal component. Thus, the PC_2 describes the largest amount of variance in the data that is not already described by PC_1. This way, for *n* dimensional data, there are *n* principal components (PCs). Each PC is orthogonal to the previous PCs and accounts for a decreasing amount of the variation in the data which is not previously accounted. Although there are *n* output bands in a PCA, the first few bands account for a high proportion of the variance in the data. In general, the first principal component PC1 collects the information that is common to all the bands used as input data in the PCA, i.e., the spatial information, while the spectral information that is specific to each band is picked up in the other principal components.

To compute a principal components transformation, a linear transformation is performed on the data meaning that the coordinates of each pixel in spectral space are recomputed using a linear equation. To perform the linear transformation, the eigenvectors and eigenvalues of the *n* principal components must be derived from the covariance matrix, as shown below:

$$D = \begin{bmatrix} D_1 & \cdots & 0 \\ \vdots & \ddots & \vdots \\ 0 & \cdots & D_n \end{bmatrix} \quad (14)$$

$$E * Cov * E^T = D \quad (15)$$

Where, E = matrix of eigenvectors, Cov = covariance matrix, T = transposition function and D = diagonal matrix of eigenvalues in which all non-diagonal elements are zeros and non-zero elements are ordered from greatest to least.

The PCA-based methods introduce less color distortion, but affect spectral responses of the multispectral data. This spectral distortion is caused due to the mismatch of overlap between the spectral responses of the multispectral image, and the bandwidth of the pan image.

Both IHS and PCA mergers are based on the same principle: to separate most of the spatial information of multispectral image from its spectral information by means of linear transforms. The IHS transform separates the spatial information of the multispectral image as the intensity (*I*) component. In the same way, PCA separates the spatial information of the image into the first principal component PC1. It is well established that PCA performs better than IHS and in particular, that the spectral distortion in the fused bands is usually less noticeable, even if it cannot be completely avoided.

3.8 Gram-Schmidt (GS) Method

The GS orthogonalization procedure is the basis for defining a powerful pansharpening method. Since GS is a generalization of PCA, in which PC1 may be arbitrarily chosen and the remaining components are calculated to be orthogonal/uncorrelated to one another and to PC1.

Like IHS and PCA method, this method also requires forward and backward transformation of MS image [39]. IHS transformation or the Brovey method work for up to three MS bands only. This drawback is outwitted in this method which is also offered by standard software packages e.g. ENVI, ESRI, etc. The Gram-Schmidt pan-sharpen method in a nutshell has following steps:

1. Compute a simulated low resolution PAN band as a linear combination of the n MS bands.

$$PAN_{sim} = \sum_{k=1}^{n} w_k MS_k \quad (16)$$

2. The Gram-Schmidt transformation is performed on the simulated lower spatial resolution PAN image and the pure low spatial resolution MS band images. To do so, the simulated lower spatial resolution PAN image is employed as the first band. Here, first of all incoming bands and the arguments of the scalar products are made dc free which turns the original Gram-Schmidt scalar products into covariances, then the iterative procedure of rotating the axes for orthogonalization is same. This Gram-Schmidt forward transform de-correlates the bands.

3. The statistics of the higher spatial resolution PAN image is adjusted to match the statistics of the first transform band resulting from the Gram-Schmidt transformation to produce a modified higher spatial resolution PAN image. The modified higher spatial resolution Pan image is substituted for the first transform band resulting from the Gram-Schmidt transformation to produce a new set of transformed bands.

4. Reverse the forward Gram-Schmidt transform using the same transform coefficients, but on the high resolution bands. The result of this backward Gram-Schmidt transform is the pan-sharpened image in high resolution.

If the user don't know the spectral sensitivity of sensor, it is very difficult to compute MS to PAN weights for getting low resolution PAN image by simulation. Thus, this method lacks a clear and standard procedure to calculate MS to PAN weights. In ENVI package, the low resolution PAN image for processing in Gram Schmidt image fusion is produced either by pixel averaging of MS bands or by low pass filtering of original PAN image followed with its decimation. These two different approaches for getting low resolution PAN image shows differences in sharpness of fused result which is more noticeable for small objects appearing on a quasi-constant background. Secondly, pansharpening a small section of image which is potentially huge is a challenge without processing entire image.

3.9 Pyramid based Methods

Pyramid is a type of multi-scale signal representation, where an image is subject to repeated smoothing and subsampling. Generally, two types of pyramids are sought viz. low-pass and band-pass, where repeated smoothing of the image with an appropriate smoothing filter followed by subsampling along each coordinate direction is done. Every cycle, a smaller image with increased smoothing, but with decreased spatial sampling density is obtained. Graphically, the entire multi-scale representation look like a pyramid, with the original image on the bottom and smaller images from every cycle stacked one on another. The Pyramid-based image fusion methods, including Laplacian pyramid transform, were all developed from Gaussian pyramid transform which have been modified and widely used [40].

3.10 Wavelet Transform based Methods

A 'wavelet' as its name implies is a small wave that grows and decays essentially in a limited time period. Its use as wavelet transform is an extension of Fourier transform in many aspects and has been successfully used in image fusion. The signal here is projected on a set of wavelet functions to get best resolution without altering the spectral contents of the image [41]. This multiresolution approach is suited to different resolutions, which allows the image decomposition in different kinds of coefficients. The coefficients from different images are combined to form new coefficients, which after inverse transformation gives fused image [42]. It provides good resolution in both time and frequency domains. It is also found to have advantages over pyramid methods in terms of increased directional information, no blocking artifacts, better signal to noise ratios and improved perception [43].

A function can be called a wavelet if it satisfies two basic properties:

Its time integral must be zero i.e.

$$\int_{-\infty}^{\infty} \psi(t)dt = 0 \quad (17)$$

and square of wavelet integrated over time is unity.

$$\int_{-\infty}^{\infty} \psi^2(t)dt = 1 \quad (18)$$

A family of wavelets can be generated by dilating and translating the mother wavelet which is given by

$$\psi_{a,b}(x) = \frac{1}{\sqrt{a}} \psi\left(\frac{x-b}{a}\right) \quad (19)$$

Here, a is the scale parameter and b is the shift parameter.

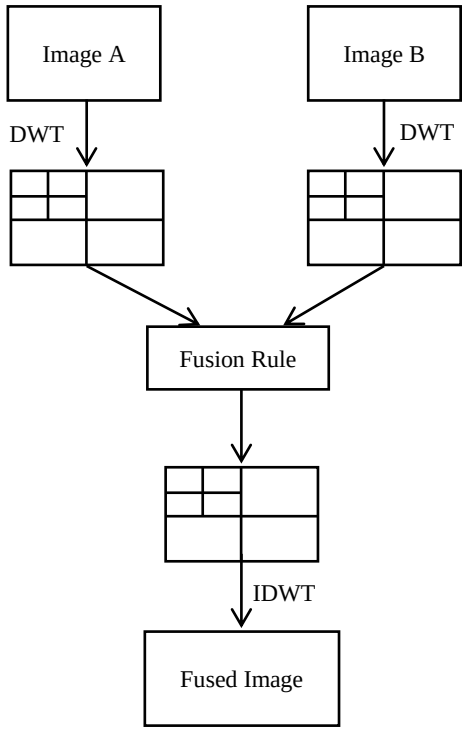

Fig 5: Image fusion using wavelet transform.

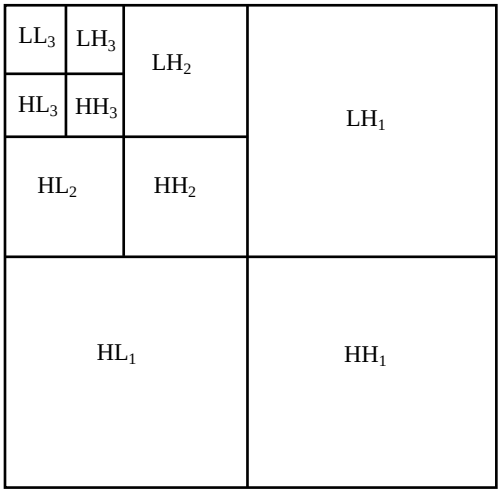

Fig 6: Decomposition of image up to 3 stages using wavelet transform.

3.11 Curvelet Transform

Enhancing the edges of image is an effective means of enhancing spatial resolution. It is observed that, the results of most wavelet-based methods of image fusion generally have a spatial resolution less than that obtained via the Brovey, IHS and PCA methods. Thus to enhance spatial resolution, the curvelet transform which represents edges better than wavelets, is also used for image fusion. Here, curvelets are seen as an extension of wavelets for multidimensional data. The key difference between the wavelet and curvelet in other words is that curvelets are really directional. Curvelets satisfy the anisotropic scaling relation *width* ≈ *length*^{2} in the spatial domain. It would take many wavelet coefficients to accurately represent a curve, while curvelets can represent a smooth contour with much fewer coefficients for the same precision. Yan Sun *et al.* in [43] analyzed the characteristics of second generation curvelet transform and proposed image fusion method in a try comprising advantages of wavelet as well as curvelet transform. Myungjin Choi *et al.* [44] also used curvelet based image fusion method to merge Landsat PAN and MS images.

3.12 Contourlet Transform

Compared to Wavelet transform, Contourlet transform has the potential to consider precise selection of the details in the PAN image, due to its anisotropic character. The images containing contours and curves are represented specifically through the use of coefficients corresponding to lines [45]. Contourlet transform consists of two steps. The initial one is to decompose image into low and high-frequency components, followed by detection of high-frequency image components using lines. The latter step is carried out by first rotating high-frequency components and then applying specific filter banks. The number of degrees between each rotation for each step can be adjusted. In wavelets, however, the image is assumed to be piecewise smooth, which is not the case here. This means that an image is made up of local information, as determined by the length of the applied filter [46].

Apart from all the approaches of image fusion discussed so far, Artificial Neural Networks (ANNs) have also proven their powerful potential because of self-adaptive nature to traditional linear and simple nonlinear analyses. The image fusion methods suits different applications and their performance is generally evaluated using some parameters called ‘Quality Metrics’ discussed in following section.

4. QUALITY METRICS

For the evaluation of image fusion result, the most addressed problem is the absence of reference image. In order to circumvent this problem, two assessment procedures may be followed viz. reduced resolution assessment and full resolution validation [9]. The first procedure considers the images at a lower spatial resolution than the original image and uses the original MS image as a reference. This procedure with some established indexes allows for a precise evaluation of the results, but there might be mismatches between the performances obtained at reduced resolution and at the original scale. Actually, the performances are related to the way with resolution degradation is performed [39]. The second approach uses quality indexes that do not require a reference image but operate on the relationships among the original images and the pansharpened result. Here, operations directly on the data at the native scale are carried, but it is biased by the definitions of the indexes. Because of the suboptimality of evaluation procedures, evaluation of the results through visual inspection is still necessary. The image quality indexes following these assessment procedures are majorly belonging to the field of information theory. They are explained in brief as follow –

4.1 Entropy (H)

The image entropy is an important indicator for measuring the image information richness. The amount of image information is bound to be changed which is fused before and after. According to the principle of Shannon information theory, an image’s information entropy is shown by –

$$H = -\sum_{i=0}^{L-1} p(i) \log_2 p(i) \qquad (20)$$

Where, $p(i)$ is the probability of grey level i, L is image’s total gray level and the dynamic range of analyzed image is $[0, L-1]$. If the value of entropy becomes higher after fusing, it indicates that the information increases and the fusion performances are improved [6] [44].

4.2 Mutual Information (MI)

Mutual information gives the measure of information from source image to the fused result. If the value of this objective indicator is greater, then richer is the fused image in terms of information. Generally, MI between two random variables is given by –

$$MI_{XY}(x,y) = \sum_{x,y} P_{XY}(x,y) log \frac{P_{XY}(x,y)}{P_X(x)P_Y(y)} \quad (21)$$

Where, X and Y are the random variables with corresponding marginal probability distributions $P_X(x)$ and $P_Y(y)$ respectively. While $P_{XY}(x,y)$ is unite probability density [6].

4.3 Correlation Coefficient (CC)

Correlation coefficient indicates degree of correlation between the original and fused images [34]. It is calculated by –

$$CC = \frac{\sum_{i=1}^{M}\sum_{j=1}^{N}[F(i,j)-\bar{F}][X(i,j)-\bar{X}]}{\sqrt{\sum_{i=1}^{M}\sum_{j=1}^{N}[F(i,j)-\bar{F}]^2 \sum_{i=1}^{M}\sum_{j=1}^{N}[X(i,j)-\bar{X}]^2}} \quad (22)$$

Where, X and F denotes the source MS and the fused images with size $M \times N$ respectively. When original and fused images are identical, the value of CC approaches to one [35] [44] [48].

4.4 Standard Deviation (σ)

Standard deviation is more efficient in the absence of noise. It measures the contrast in the fused image [6] [34]. An image with high contrast would have a high standard deviation given by –

$$\sigma = \sqrt{\sum_{i=o}^{L}(i-i')^2 h_{If}(i), \dots i'} = \sum_{i=0}^{L} i h_{If} \quad (23)$$

Where, $h_{If}(i)$ is the normalized histogram of the fused image $I_f(x,y)$ and L is the number of frequency bins in histogram.

4.5 Mean Square Error (MSE)

The mathematical equation of MSE is given by –

$$MSE = \frac{1}{mn}\sum_{i=1}^{m}\sum_{j=1}^{n}\left(A_{ij} - B_{ij}\right)^2 \quad (24)$$

Where, A is the reference image, B is the fused image to be assessed, i is the pixel row index, j is the pixel column index, m is number of rows and n is number of columns [6].

4.6 Root Mean Square Error (RMSE)

The RMSE is another standard measure of difference between the reference image and the fused image [34] given by –

$$RMSE = \left(\frac{\sum_{i=1}^{M}\sum_{j=1}^{N}[I_R(i,j)-I_F(i,j)]^2}{M \times N}\right)^{\frac{1}{2}} \quad (25)$$

Where, $I_R(i,j)$and $I_F(i,j)$are the image pixel values of the reference image and the fused image respectively. $M \times N$ is the image size. Greater the RMSE, higher the difference between reference and fused image will be. The main drawback of RMSE is that errors in each band are not related to the mean value of the band itself [6] [9] [42] [48].

4.7 Relative Average Spectral Error (RASE)

To estimate the global spectral quality of the fused images, the index of the RASE is expressed as a percentage. This percentage characterizes the average performance of the method of image fusion in the spectral bands considered [35] [44], given by –

$$RASE = \frac{100}{M}\sqrt{\frac{1}{N}\sum_{i=1}^{N} RMSE^2(B_i)} \quad (26)$$

Where, M is the mean radiance of the N spectral bands (B_i) of the original MS bands, and $RMSE$ is root mean square error computed [34].

4.8 Errur Relative Globale Adimensionnelle de Synthèse (ERGAS)

It means the relative global dimensional synthesis error. It is a more credited global index proposed for pansharpening as follows:

$$ERGAS = \frac{100}{R}\sqrt{\frac{1}{N}\sum_{k=1}^{N}\left(\frac{RMSE(I_k,J_k)}{\mu(I_k)}\right)^2} \quad (27)$$

Where RMSE is defined as (25) and μ denotes mean of the image. Since ERGAS is composed by a sum of RMSE values, smaller ERGAS indicates better fusion results and its optimal value is 0 [9] [34] [35] [39] [44] [48].

4.9 Peak to Peak Signal to Noise Ratio (PSNR)

PSNR is the ratio between the maximum possible power of a signal and the power of corrupting noise that affects the fidelity of its representation. The PSNR measure is given by –

$$PSNR(dB) = 20 \log \frac{255\sqrt{3MN}}{\sqrt{\sum_{i=1}^{M}\sum_{j=1}^{N}(B'(i,j)-B(i,j))^2}} \quad (28)$$

Where, B is the reference image, B' is the fused image to be assessed, i is the pixel row index, j is the pixel column index, M is number of rows and N is the number of columns [6] [42].

4.10 Universal Image Quality Index (UIQI) or Q - index

It is a scalar index which overcomes some limitations of RMSE. It is given by –

$$Q(I,J) = \frac{\sigma_{IJ}}{\sigma_I \sigma_J} \cdot \frac{2\bar{I}\bar{J}}{(\bar{I})^2+(\bar{J})^2} \cdot \frac{2\sigma_I\sigma_J}{(\sigma_I^2+\sigma_J^2)} \quad (29)$$

Where, σ_{IJ} is sample covariance of I and J, while $\bar{I}$ is sample mean of I. It varies in the range$[-1,1]$, with 1 denoting the best fidelity to reference. The vector expansion of Q-index to vector data up to four bands accounting for spectral distortion is Q4 vector index. The Q4 index takes values in [0,1] with one being the best value [4] [9].

4.11 Spatial Frequency (SF)

Spatial frequency is used to measure the overall activity level of an image [9], which is defined as –

$$SF = \sqrt{(RF)^2 + (CF)^2} \quad (30)$$

Where RF and CF are row frequency and column frequency respectively.

$$RF = \sqrt{\frac{1}{MN}\sum_{i=1}^{M}\sum_{j=2}^{N}[I(i,j)-I(i,j-1)]^2} \quad (31)$$

$$CF = \sqrt{\frac{1}{MN}\sum_{i=1}^{M}\sum_{j=2}^{N}[I(i,j)-I(i-1,j)]^2} \quad (32)$$

4.12 Spectral Angle Mapper (SAM)

The Spectral Angle Mapper (SAM) reflects the global measurement of spectral distortion by averaging whole image [39] [48]. It consists of calculating the angle between the

corresponding pixels of the fused and reference images in the space defined by considering each spectral band as a coordinate axis. Let, $I_{\{n\}} = [I_{1,\{n\}}, \dots, I_{N,\{n\}}]$ be a pixel vector of the MS image I with N bands, the SAM between $I_{\{i\}}$ and $J_{\{i\}}$is defined as follows:

$$SAM(I_{\{i\}}, J_{\{i\}}) = arccos\left(\frac{\langle I_{\{i\}}, J_{\{i\}}\rangle}{\|I_{\{i\}}\|\|J_{\{i\}}\|}\right) \quad (33)$$

Where, $\langle I_{\{i\}}, J_{\{i\}}\rangle$ denotes the scalar product and $\|I_{\{i\}}\|$ denotes vector l-2 norm. The optimum value of SAM equal to zero denotes absence of spectral distortion, but radiometric distortion is possible (i.e. the two pixel vectors are parallel but have different lengths) [9].

SAM is further improved to Expanded Spectral Angle Mapper (ESAM) which is more sensitive to difference between two images, because the value of the ESAM will be equal to 0 only for two identical images whereas the values of the SAM can be equal to 0 for two similar images. The ESAM measures information from isolated pixels only, and does not consider the neighboring pixel relationships, which are more important for structures and textures [47].

4.13 Quality w/no reference (QNR)

It is defined as –

$$QNR = (1 - D_\lambda)^\alpha (1 - D_S)^\beta \quad (34)$$

It is thus composed by the product, weighted by the coefficients α and β, of two separate values D_λ and D_S, which quantify the spectral and the spatial distortion, respectively. The higher the QNR index, the better the quality of the fused product. The maximum theoretical value of this index is 1, when both D_λ and D_S are equal to 0.

The spectral distortion is estimated by

$$D_\lambda = \sqrt[p]{\frac{1}{N(N-1)}\sum_{i=1}^{N}\sum_{j=1, j\neq i}^{N}\left|d_{i,j}(MS, \widehat{MS})\right|^p} \quad (35)$$

Where, $d_{i,j}(MS, \widehat{MS}) = Q(MS_i, MS_j) - Q(\widehat{MS_i}, \widehat{MS_j})$

The Q-index is used to calculate the dissimilarities between couples of bands, and the parameter p is typically set to one.

The spatial distortion is calculated by

$$D_S = \sqrt[q]{\frac{1}{N}\sum_{i=1}^{N}\left|Q(\widehat{MS_i}, P) - Q(MS_i, P_{LP})\right|^q} \quad (36)$$

The P_{LP} is a low-resolution PAN image at the same scale of MS image and q is usually set to one. From a practical point of view, the perfect alignment between the interpolated version of the MS and the PAN images should be assured, to avoid the loss of meaning for this quality index [9] [48].

5. FUTURE SCOPE & LIMITATIONS

Many research papers have reported the limitations of existing fusion techniques. The most significant problems are color distortion, operator's fusion experience, the data set being fused, capacity of satellite sensor to store image data, etc. No automatic solution has been achieved to consistently produce high quality fusion for different data sets. To reduce the color distortion and improve the fusion quality, a wide variety of strategies have been developed, each specific to a particular fusion technique or image set.

The satellites used from past decades are allocated the frequency band of visible spectrum region. Today, with increase in number of satellites launched by different nations, newer satellites are being assigned frequency bands of near infra-red region. This makes quality difference in imagery captured by older satellites and newer satellites. Hence, image fusion techniques give different results for imagery of newer satellites and old satellites. It is observed that, when traditional fusion and adjustment techniques are used with this imagery, captured by newer satellites, color distortion becomes a significant problem.

Therefore, all the limitations of existing image fusion methods including color distortion for the above said reason gives motivation for development of new improved image fusion method which will compensate these limitations.

6. CONCLUSION

In this paper, we discussed different image fusion levels, current state of art of image fusion in remote sensing, different image fusion methods and image fusion evaluation parameters. Concluding remarks for all these sections are organized as follow:

- Image fusion methods obtain more accurate and reliable image information by eliminating redundancy.
- Analysis of some researchers shows that different image fusion methods suits different applications.
- The pixel level fusion has been extensively researched for different approaches, since it gives comparatively better quality of fused results; but at the expense of more time consumption.
- For evaluation of image fusion algorithms, there is no standardized reference hence common practice followed is to test the algorithms on more number of datasets and to use optimum fusion strategy depending on application.
- Along with the objective evaluation, many times it is reported that the fused result should be subjectively evaluated based on visual characteristics.

REFERENCES

[1] John A. Richards, "Remote Sensing Digital Image Analysis", *Springer, ISBN-13 978-3-540-25128-6,* 2006

[2] H.B. Mitchell, "Image Fusion: Theories, Techniques And Applications", *Springer-Verlag Berlin Heidelberg, e-ISBN 978-3-642-11216-4,* 2010

[3] Yufeng Zheng, "Image Fusion And Its Applications", *InTech Publication, ISBN 978-953-307-182-4,* May 2011

[4] Zhijun Wang, Djemel Ziou, Costas Armenakis, Deren Li and Qingquan Li, "A Comparative Analysis of Image Fusion Methods", *IEEE Transactions on Geoscience And Remote Sensing,* Vol. 43, No. 6, June 2005, pp. 1391 – 1402

[5] Veeraraghavan Vijayaraj, Nicolas H. Younan and Charles G. O'Hara, "Concepts of Image Fusion in Remote Sensing Applications", *IEEE,* Geoscience and Remote Sensing International Symposium - IGARSS, 2006, pp. 3781 – 3784

[6] Tian Hui and Wang Binbin, "Discussion and Analyze on Image Fusion Technology", *IEEE, Second International Conference on Machine Vision (ICMV'09),* 2009, pp. 246 – 250

[7] Zhao Dawei and Zi Fang, "A New Improved Hierarchical Model of Image Fusion", *IEEE, The Eighth International Conference on Electronic Measurement and Instruments, ICEMI'2007,* pp – 2-853 to 2-857

[8] Zhihui Wang, Yang Tie and Yueping Liu, "Design and Implementation of Image Fusion System", *IEEE, International Conference on Computer Application and System Modeling (ICCASM)*, 2010, pp – V10-140 to V10-143

[9] Gemine Vivone, Luciano Alparone, Jocelyn Chanussot, Mauro Dalla Mura, Andrea Garzelli, Giorgio A. Licciardi, Rocco Restaino and Lucien Wald, "A Critical Comparison Among Pansharpening Algorithms", *IEEE Transactions on Geoscience and Remote Sensing*, Vol. 53, No. 5, May 2015, pp. 2565 – 2586

[10] Wenqing Wang, Licheng Jiao and Shuyuan Yang, "Novel Adaptive Component-Substitution-Based Pan-Sharpening Using Particle Swarm Optimization", *IEEE Geoscience And Remote Sensing Letters*, Vol. 12, No. 4, April 2015, pp. 781 – 785

[11] Andrea Garzelli, "Pansharpening of Multispectral Images Based on Nonlocal Parameter Optimization", *IEEE Transactions on Geoscience and Remote Sensing*, Vol. 53, No. 4, April 2015, pp. 2096 – 2107

[12] Qizhi Xu, Yun Zhang, Bo Li and Lin Ding, " Pansharpening Using Regression of Classified MS and Pan Images to Reduce Color Distortion", *IEEE Geoscience And Remote Sensing Letters*, Vol. 12, No. 1, January 2015, pp. 28 – 32

[13] Hamid Reza Shahdoosti and Hassan Ghassemian, "Fusion of MS and PAN Images Preserving Spectral Quality", *IEEE Geoscience And Remote Sensing Letters*, Vol. 12, No. 3, March 2015, pp. 611 – 615

[14] Abdelaziz Kallel, "MTF-Adjusted Pansharpening Approach Based on Coupled Multiresolution Decompositions", *IEEE Transactions on Geoscience and Remote Sensing*, Vol. 53, No. 6, June 2015, pp. 3124 – 3145

[15] Kishor P. Upla Manjunath V. Joshi and Prakash P. Gajjar, "An Edge Preserving Multiresolution Fusion: Use of Contourlet Transform and MRF Prior", *IEEE Transactions on Geoscience and Remote Sensing*, Vol. 53, No. 6, June 2015, pp. 3210 – 3220

[16] Gemine Vivone, Miguel Simões, Mauro Dalla Mura, Rocco Restaino, José M. Bioucas-Dias, Giorgio A. Licciardi and Jocelyn Chanussot, "Pansharpening Based on Semiblind Deconvolution", *IEEE Transactions on Geoscience and Remote Sensing*, Vol. 53, No. 4, April 2015, pp. 1997 – 2010

[17] Syed Muhammad Umer Abdullah, Naveed ur Rehman, Muhammad Murtaza Khan and Danilo P. Mandic, "A Multivariate Empirical Mode Decomposition Based Approach to Pansharpening", *IEEE Transactions on Geoscience and Remote Sensing*, Vol. 53, No. 7, July 2015, pp. 3974 – 3984

[18] Huihui Song, Bo Huang, Qingshan Liu and Kaihua Zhang, " Improving the Spatial Resolution of Landsat TM/ETM+ Through Fusion With SPOT5 Images via Learning-Based Super-Resolution", *IEEE Transactions on Geoscience and Remote Sensing*, Vol. 53, No. 3, March 2015, pp. 195 – 1204

[19] Maria Rosaria Vicinanza, Rocco Restaino, Gemine Vivone, Mauro Dalla Mura and Jocelyn Chanussot, "A Pansharpening Method Based on the Sparse Representation of Injected Details", *IEEE Geoscience And Remote Sensing Letters*, Vol. 12, No. 1, January 2015, pp. 180 – 184

[20] Miguel Simões, José Bioucas-Dias, Luis B. Almeida and Jocelyn Chanussot, "A Convex Formulation for Hyperspectral Image Superresolution via Subspace-Based Regularization", *IEEE Transactions on Geoscience and Remote Sensing*, Vol. 53, No. 6, June 2015, pp. 3373 – 3388

[21] Xuejian Sun, Lifu Zhang, Hang Yang, Taixia Wu, Yi Cen and Yi Guo, "Enhancement of Spectral Resolution for Remotely Sensed Multispectral Image", *IEEE Journal of Selected Topics In Applied Earth Observations And Remote Sensing*

[22] Caroline M. Gevaert, Juha Suomalainen, Jing Tang and Lammert Kooistra, " Generation of Spectral–Temporal Response Surfaces by Combining Multispectral Satellite and Hyperspectral UAV Imagery for Precision Agriculture Applications", *IEEE Journal of Selected Topics In Applied Earth Observations And Remote Sensing*

[23] Qi Wei, José Bioucas-Dias, Nicolas Dobigeon and Jean-Yves Tourneret, "Hyperspectral and Multispectral Image Fusion Based on a Sparse Representation", *IEEE Transactions on Geoscience and Remote Sensing*, Vol. 53, No. 7, July 2015, pp. 3658 – 3668

[24] Frosti Palsson, Johannes R. Sveinsson, Magnus Orn Ulfarsson and Jon Atli Benediktsson, "Model-Based Fusion of Multi- and Hyperspectral Images Using PCA and Wavelets", *IEEE Transactions on Geoscience and Remote Sensing*, Vol. 53, No. 5, May 2015, pp. 2652 - 2663

[25] Claudia Paris and Lorenzo Bruzzone, "A Three-Dimensional Model-Based Approach to the Estimation of the Tree Top Height by Fusing Low-Density LiDAR Data and Very High Resolution Optical Images", *IEEE Transactions on Geoscience and Remote Sensing*, Vol. 53, No. 1, January 2015, pp. 467 – 480

[26] Wenzhi Liao, Aleksandra Pižurica, Rik Bellens, Sidharta Gautama and Wilfried Philips, "Generalized Graph-Based Fusion of Hyperspectral and LiDAR Data Using Morphological Features", *IEEE Geoscience And Remote Sensing Letters*, Vol. 12, No. 3, March 2015, pp. 552 – 556

[27] Fatemeh Tabib Mahmoudi, Farhad Samadzadegan, and Peter Reinartz, Jr., "Object Recognition Based on the Context Aware Decision-Level Fusion in Multiviews Imagery", *IEEE Journal of Selected Topics In Applied Earth Observations And Remote Sensing* Vol. 8, No. 1, January 2015, pp. 12 – 22

[28] Gianluca Gennarelli, Moeness G. Amin, Francesco Soldovieri and Raffaele Solimene, "Passive Multiarray Image Fusion for RF Tomography by Opportunistic Sources", *IEEE Geoscience And Remote Sensing Letters*, Vol. 12, No. 3, March 2015, pp. 641 – 645

[29] Yong Xu, Bo Huang, Yuyue Xu, Kai Cao, Chunlan Guo and Deyu Meng, " Spatial and Temporal Image Fusion via Regularized Spatial Unmixing", *IEEE Geoscience And Remote Sensing Letters*, Vol. 12, No. 6, June 2015, pp. 1362 – 1366

[30] Wei Li, Chen Chen, Hongjun Su and Qian Du, "Local Binary Patterns and Extreme Learning Machine for

Hyperspectral Imagery Classification", *IEEE Transactions on Geoscience and Remote Sensing,* Vol. 53, No. 7, July 2015, pp. 3681 – 3693

[31] Zhang Yingjie and Ge Liling, "A Simple and Efficient Hybrid Image Fusion Approach", *3rd IEEE Conference on Industrial Electronics and Applications (ICIEA),* 2008, pp. 1109 – 1113

[32] Benjamin W. Martin and Ranga R. Vatsavai, "Evaluating fusion techniques for multi-sensor satellite image data", *Geospatial InfoFusion III, Proc. of SPIE,* Vol. 8747, 2013, pp. 1 – 8

[33] Yuhong Ding and Yanhui Wang, "Analysis and Evaluation on Fusion Methods of Medium and High Spatial Resolution Remote Sensing Image", *IEEE, 19th International Conference on Geoinformatics,* 2011, pp. 1 – 4

[34] Myungjin Choi, "A New Intensity-Hue-Saturation Fusion Approach to Image Fusion With a Tradeoff Parameter", *IEEE Transactions on Geoscience And Remote Sensing,* Vol. 44, No. 6, June 2006, pp. 1672 – 1682

[35] Heng Chu and Weile Zhu, "Fusion of IKONOS Satellite Imagery Using IHS Transform and Local Variation", *IEEE Geoscience And Remote Sensing Letters,* Vol. 5, No. 4, October 2008, pp. 653 – 657

[36] Chun-Liang Chien and Wen-Hsiang Tsai, "Image Fusion With No Gamut Problem by Improved Nonlinear IHS Transforms for Remote Sensing", *IEEE Transactions on Geoscience And Remote Sensing,* Vol. 52, No. 1, January 2014, pp. 651 – 663

[37] Changtao He, Quanxi Liu, Hongliang Li and Haixu Wang, " Multimodal medical image fusion based on IHS and PCA", *Symposium on Security Detection and Information Processing, Procedia Engineering 7, Elsevier Ltd.,* 2010, pp. 280 – 285

[38] Wenkao Yang, Jing Wang and Jing Guo, "A Novel Algorithm for Satellite Images Fusion Based on Compressed Sensing and PCA", *Hindawi Publishing Corporation, Mathematical Problems in Engineering,* Volume 2013, pp. 1 – 10

[39] Xin Huang, Dawei Wen, Junfeng Xie and Liangpei Zhang, "Quality Assessment of Panchromatic and Multispectral Image Fusion for the ZY-3 Satellite: From an Information Extraction Perspective", *IEEE Geoscience And Remote Sensing Letters,* Vol. 11, No. 4, April 2014, pp. 753 – 757

[40] M. Pradeep, "Implementation of Image Fusion algorithm using MATLAB (LAPLACIAN PYRAMID)", *IEEE, International Multi-Conference on Automation, Computing, Communication, Control and Compressed Sensing (iMac4s),* 2013, pp. 165 – 168

[41] Hui Lee, B.S. Manjunath and Snjeet k. Mitra, "Multi-Sensor Image Fusion Using The Wavelet Transform", *IEEE, International Conference on Image Processing (ICIP-94),* 1994, pp. 51 – 55

[42] Anna Wang, Haijing Sun and Yueyang Guan, "The Application of Wavelet Transform to Multi-modality Medical Image Fusion", *IEEE, International Conference on Networking, Sensing and Control (ICNSC'06),* 2006, pp. 270 – 274

[43] Yan Sun, Chunhui Zhao and Ling Jiang, "A New Image Fusion Algorithm Based on Wavelet Transform and the Second Generation Curvelet Transform", *IEEE, International Conference on Image Analysis and Signal Processing (IASP),* 2010, pp. 1 – 4

[44] Myungjin Choi, Rae Young Kim, Myeong-Ryong Nam and Hong Oh Kim, "Fusion of Multispectral and Panchromatic Satellite Images Using the Curvelet Transform", *IEEE Geoscience And Remote Sensing Letters,* Vol. 2, No. 2, April 2005, pp. 136 – 140

[45] LIU Fu, LI Jin and Huang Caiyun, "Image Fusion Algorithm Based on Simplified PCNN in Nonsubsampled Contourlet Transform Domain", *International Workshop on Information and Electronics Engineering (IWIEE), Procedia Engineering 29, Elsevier Ltd.,* 2012, pp. 1434 – 1438

[46] Saad M. Darwish, "Multi-level fuzzy contourlet-based image fusion for medical applications", *IET Image Processing,* Volume 7, Issue 7, ISSN 1751-9659, 2013, pp. 694 – 700

[47] Shaohui Chen, Hongbo Su, Renhua Zhang, Jing Tian and Lihu Yang, "The Tradeoff Analysis for Remote Sensing Image Fusion Using Expanded Spectral Angle Mapper", *Sensors, ISSN 1424-8220,* January 2008, pp. 520 – 528

[48] Shutao Li, Haitao Yin and Leyuan Fang, "Remote Sensing Image Fusion via Sparse Representations Over Learned Dictionaries", *IEEE Transactions on Geoscience And Remote Sensing,* Vol. 51, No. 9, September 2013, pp. 4779 – 4789